Environmental Science & Technology

Article

pubs.acs.org/est

An X-ray Photoelectron Spectroscopy Study of Surface Changes on Brominated and Sulfur-Treated Activated Carbon Sorbents during Mercury Capture: Performance of Pellet versus Fiber Sorbents

Arindom Saha,[†] David N. Abram,[†] Kendra P. Kuhl,[‡] Jennifer Paradis,[∥] Jenni L. Crawford,[∥] Erdem Sasmaz,[§] Ramsay Chang,[⊥] Thomas F. Jaramillo,*[,†] and Jennifer Wilcox*[,§]

[†]Department of Chemical Engineering, Stanford University, Stanford, California 94305, United States

[‡]Department of Chemistry, Stanford University, Stanford, California 94305, United States

[§]Department of Energy Resources Engineering, Stanford University, Stanford, California 94305, United States

[∥]URS Corporation, 9400 Amberglen Boulevard, Austin, Texas 78729, United States

[⊥]Electric Power Research Institute, 3412 Hillview Avenue, Palo Alto, California 94304, United States

Supporting Information

ABSTRACT: This work explores surface changes and the Hg capture performance of brominated activated carbon (AC) pellets, sulfur-treated AC pellets, and sulfur-treated AC fibers upon exposure to simulated Powder River Basin-fired flue gas. Hg breakthrough curves yielded specific Hg capture amounts by means of the breakthrough shapes and times for the three samples. The brominated AC pellets showed a sharp breakthrough after 170−180 h and a capacity of 585 μg of Hg/g, the sulfur-treated AC pellets exhibited a gradual breakthrough after 80−90 h and a capacity of 661 μg of Hg/g, and the sulfur-treated AC fibers showed no breakthrough even after 1400 h, exhibiting a capacity of >9700 μg of Hg/g. X-ray photoelectron spectroscopy was used to analyze sorbent surfaces before and after testing to show important changes in quantification and oxidation states of surface Br, N, and S after exposure to the simulated flue gas. For the brominated and sulfur-treated AC pellet samples, the amount of surface-bound Br and reduced sulfur groups decreased upon Hg capture testing, while the level of weaker Hg-binding surface S(VI) and N species (perhaps as NH_4^+) increased significantly. A high initial concentration of strong Hg-binding reduced sulfur groups on the surface of the sulfur-treated AC fiber is likely responsible for this sorbent's minimal accumulation of S(VI) species during exposure to the simulated flue gas and is linked to its superior Hg capture performance compared to that of the brominated and sulfur-treated AC pellet samples.

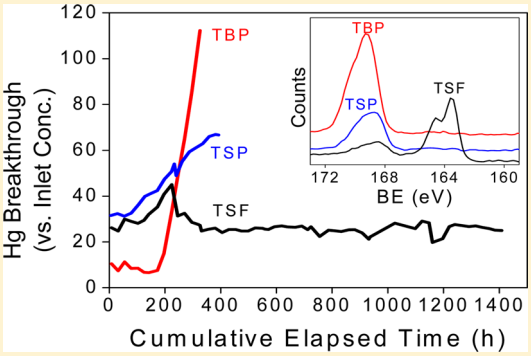

INTRODUCTION

Hg is a toxic pollutant that can cause a variety of serious health problems depending on its chemical form. Methylmercury (MeHg) is an insoluble form of Hg that is known to accumulate in fish through the food chain. Ingesting contaminated fish can severely impair the neurological and cognitive development of infants and children.[1] MeHg accumulates in fish because of a combination of natural and anthropogenic emissions. Approximately half of these emissions are anthropogenic, with the largest source (~45%) being fossil fuel combustion, primarily from coal.[2] To reduce anthropogenic Hg emissions, the Environmental Protection Agency (EPA) issued the Mercury and Air Toxics Standards in December 2011, requiring a 91% removal of Hg for existing coal power plants and higher levels of removal for new plants.[1] The technology for meeting these goals currently exists, but several methods are being explored and optimized to maximize Hg capture rates while minimizing the impact on the cost of electricity.

Existing emission controls for other coal combustion pollutants such as NO_x, SO_x, and particulates can also be used to capture a portion of the released Hg.[3] Without the addition of any Hg emission control, an average of ~33% of the released Hg is captured.[4] Particle-bound Hg can be captured using either an electrostatic precipitator (ESP) or a fabric filter (FF), oxidized Hg may be removed using wet flue gas desulfurization (FGD), and a portion of the elemental Hg can be oxidized using selective catalytic reduction (SCR) for improved removal during FGD. The combination of FGD and SCR is able to remove 89% of the Hg.[5] Injecting sorbent

Received: August 5, 2013
Revised: November 1, 2013
Accepted: November 1, 2013
Published: November 21, 2013

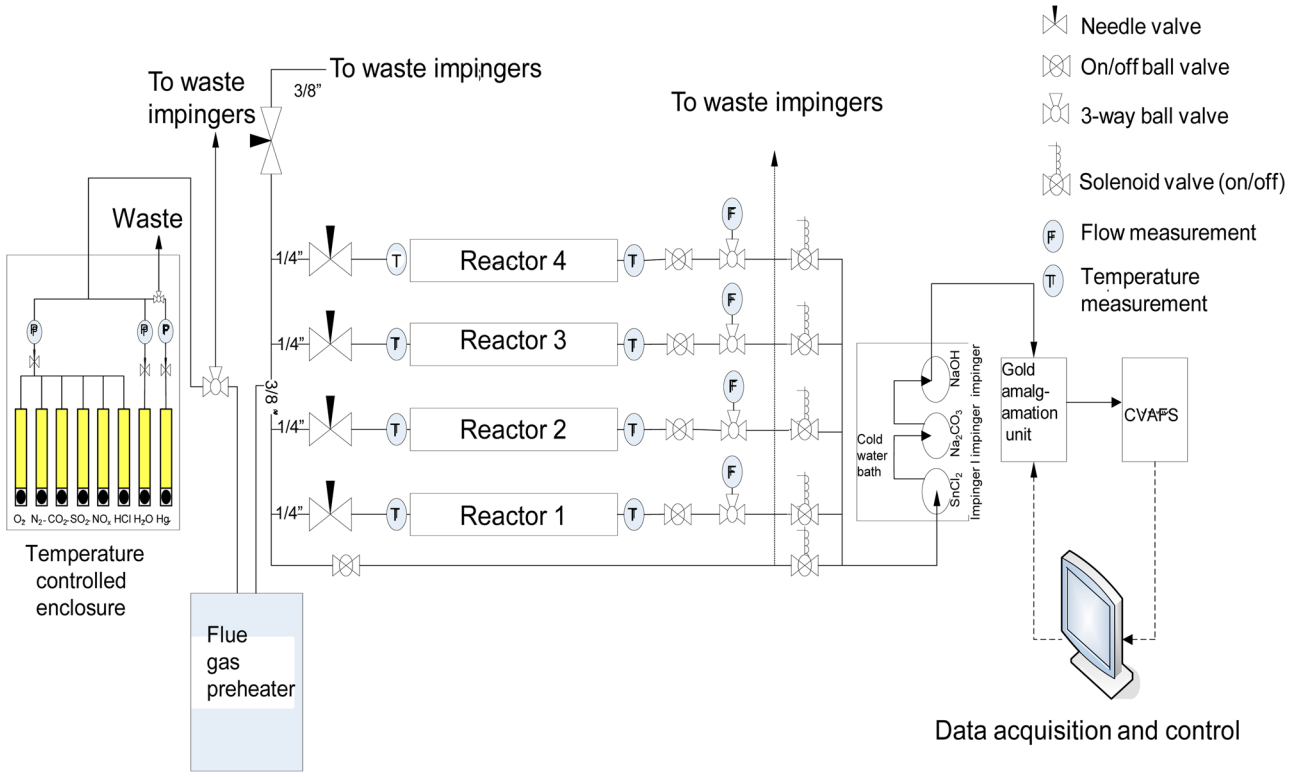

Figure 1. Schematic of the bench-scale test system used at URS Corp.

upstream of an ESP or FF is another effective approach to oxidizing and retaining the volatile Hg^0,[6] but use of the most common sorbent, activated carbon (AC), can be fairly expensive. The removal of Hg from a 500 MWe coal power plant can cost $1−10 million/year and cause fly ash to be unfit to sell for concrete production.[4,7] For this reason, improved and cheaper sorbents such as functionalized AC carbon are being explored. While functionalizing the AC sorbent surfaces with halogens or sulfur typically improves Hg capture performance,[8−12] the mechanism for the improved capture of Hg is not entirely understood.

To improve our understanding of how the capture of Hg by AC sorbents is related to acid gas concentrations in the flue gas, Olson et al.[13] used X-ray photoelectron spectroscopy (XPS) to study the surface chemistry of AC in low-HCl (<200 ppm) simulated flue gas. Similar XPS studies were also performed on lignite AC by Laumb et al.[14] and on brominated AC by Hutson et al.[12] to understand the effect of flue gas components on the sorbent surface chemistry. Via combination of observations from bench-scale tests and XPS studies, it appears that the presence of both SO_2 and NO_x in the flue gas mixture leads to rapid breakthrough of Hg, indicating poor Hg capture.[15]

This investigation reflects a comprehensive sorbent bench-scale testing and characterization study of Hg removal in simulated Powder River Basin (PRB) fired flue gas by three modified AC sorbents: brominated AC pellets, sulfur-treated AC pellets, and sulfur-treated AC fiber sorbents. Hg equilibrium adsorption capacity tests were performed for each sample using identical flue gas conditions. Hg breakthrough curves measuring the Hg concentration at the outlet of the sorbent bed over time were obtained for each capacity test. XPS studies were conducted for each sorbent before and after Hg adsorption tests to identify the changes in the AC surface chemistry resulting from exposure to the flue gas. This study aims to identify changes in the surface chemistry of the different modified AC sorbents upon exposure to similar Hg capture conditions and offers insight into their Hg capture mechanisms.

EXPERIMENTAL SECTION

Three distinct AC sorbents were tested at URS Corp. for Hg capture under the simulated PRB-fired flue gas conditions: brominated AC pellets, sulfur-treated AC pellets, and sulfur-treated AC fibers. The tested samples will be termed tested brominated pellets (TBP), tested sulfur-treated pellets (TSP), and tested sulfur-treated fibers (TSF). Untested samples, which were not exposed to simulated flue gases, will be termed untested brominated pellets (UTBP), untested sulfur-treated pellets (UTSP), and untested sulfur-treated fibers (UTSF). The two pelletized samples are commercially available and are 3 mm in diameter, while the sulfur-treated fiber sample was prepared by M. Rostam-Abadi's group at the University of Illinois at Urbana-Champaign (Urbana, IL). The fiber samples were prepared by impregnating elemental sulfur followed by heat treatments.[16]

All bench-scale Hg adsorption tests were conducted at URS Corp.'s Process Technologies Office in Austin, TX. The schematic design of the test unit is shown in Figure 1. The flue gas mixture used for testing contained 12−17 μg of Hg/Nm^3, 50 ppm SO_2, 400 ppm NO_x (95% NO), 12% H_2O, 12% CO_2, 6% O_2, and 70% N_2; the mixture did not contain any HCl. All samples were tested at 145 °F. These conditions simulate the flue gas downstream of a wet FGD system at a PRB-fired coal plant. Hg was added to the flue gas by flowing a nitrogen carrier stream through a temperature-controlled permeation chamber containing the Hg^0. More detailed information with regard to bench-scale testing, sorbent configuration, and Hg adsorption test results is provided in the Supporting

Information. Figures S1 and S2 depict the mode of packing of the pelletized and fiber samples, respectively.

All samples were analyzed by XPS at the Stanford Nanocharacterization Laboratory (SNL) at Stanford University. The PHI 5000 Versa Probe Scanning XPS Microprobe used for analysis is equipped with a 350 W monochromatic Al Kα X-ray source (1486.6 eV) and is operated at a base pressure of $\sim 5 \times 10^{-10}$ Torr. The X-rays are focused onto a spot size of 100 μm $\times$ 800 μm on each sample. The detection limits of the instrument were approximately 1% on the surface (0.01 monolayer) and ~0.1% in the bulk. The AC pellets were mounted on double-sided Scotch tape on a clean sample holder without any further preparation prior to XPS analysis, while the AC fiber was mounted directly onto a clean sample holder and analyzed under identical conditions. All survey and high-resolution scans were taken with the charge neutralizer operating at 30 V to avoid any charging caused by any insulating components of the sample such as the glass wool residue.

RESULTS AND DISCUSSION

Hg Adsorption Tests Using a Bench-Scale Testing System. Figure 2 exhibits the Hg breakthrough curves

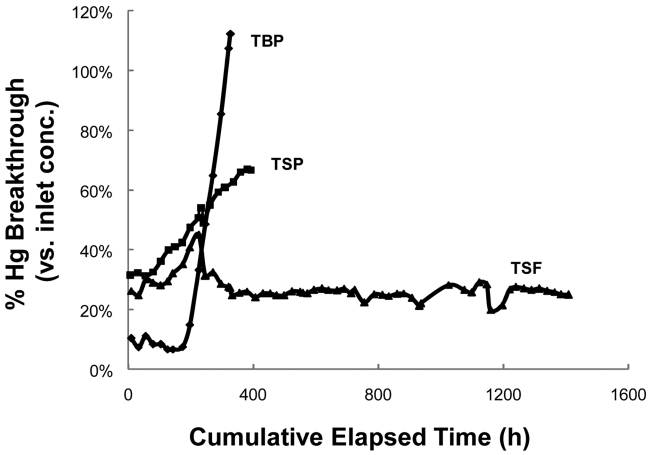

Figure 2. Compiled breakthrough curves for all tested samples.

obtained from Hg equilibrium adsorption capacity testing of the pellet and fiber AC sorbents. Key data pertaining to these experiments are listed in Table 1. The TBP had an initial Hg breakthrough of approximately 10%, indicating that the sample was capable of removing 90% of the Hg in the simulated flue gas. After 170–180 h, the amount of Hg breakthrough increased steeply to 100%, indicating that an equilibrium coverage of Hg had been reached. A normalized Hg capacity of 585 μg/g of carbon (at an inlet concentration of 50 μg of Hg/Nm^3)[17] was calculated using TBP breakthrough data. The TSP had a higher initial breakthrough of approximately 30%, and after only 80–90 h it increased gradually, suggesting that the active adsorption sites on it were less efficient in Hg capture than the TBP. The test was stopped after 400 h, and a normalized Hg capacity of 661 μg/g (at an inlet concentration of 50 μg of Hg/Nm^3) for the TSP sample was observed.

Table 1. Test Results of the Samples Exposed to the Simulated Flue Gases

sample name	sample type	inlet Hg concentration (μg/Nm^3)	normalized capacity (μg/g at 50 μg of Hg/Nm^3)	face velocity (fps)
TBP	pellet	16.9	585	2.5
TSP	pellet	12.1	661	2.5
TSF	fiber	12.4	>9700	1.1

The TSF sample was exposed to the same flue gas and had an initial breakthrough of ~25% that could suggest that it is less efficient at Hg capture than the TBP sample, that there was poor mass transfer from the flue gas matrix to the interiors of the AC fibers, or that there were channeling effects, though care was taken to prevent channeling (see the Supporting Information). Aside from a temporary excursion to 45% breakthrough, likely caused by an upset in the test system, the initial breakthrough level was maintained for 1400 h (approximately 8 weeks) until the test was finally terminated. The TSF sorbent performed exceptionally well, and at the time the test was stopped, it showed a normalized Hg capacity of >9700 μg/g of carbon (at an inlet concentration of 50 μg of Hg/Nm^3), far exceeding the capacity of either the TBP or TSP. The surface area of the AC fiber is 438 m^2/g, so it is unlikely that the 20-fold difference (or greater) in capacity is due to the difference in surface areas of the pellet and fiber sorbents. To help explain this large difference in performance, XPS was used to gain a view of the surface chemistry before and after Hg capture.

X-ray Photoelectron Spectroscopy. The elemental compositions of all samples before and after testing (Table 2) were obtained from their survey spectra (Figure S3 of the Supporting Information). To facilitate quantitative comparisons among samples, peak areas were normalized to the peak area of the C 1s line, as shown in Table 3. High-resolution scans were also taken for each element present to obtain information about their oxidation states. All samples contained a strong C 1s peak from the inherent sorbent material, which was shifted to 284.5 eV to calibrate the spectra,[18] and had a tail extending toward higher binding energies indicative of either oxidized or adventitious carbon (Figure S4 of the Supporting Information). The brominated and sulfur-treated pellets contained aluminum, silicon, calcium, and sodium in small amounts, from trace to 2.0 atom % (Figures S5–S7 of the Supporting Information). Their presence is not surprising as these elements are naturally occurring and found in activated carbons.[19] The corresponding quantitative values of these elements obtained from high-resolution spectra are compiled in Table S1 of the Supporting Information. None of these impurities were present in the UTSF sample, which was possibly synthesized using a different AC precursor.

Hg lines were not observed in any scans, indicating that the concentration of Hg was below the XPS detection limits for all samples. This was not entirely unexpected as the surface concentrations of Hg calculated from breakthrough curve data, even for the high-capacity TSF sample, were expected to be below the XPS detection limits (see the Supporting Information). Possible Hg desorption under UHV conditions presents additional difficulties as does interference between the Hg 4f doublet at 101 eV/105 eV[20,21] and the broad Si 2p peaks from SiO_x at 102–103 eV[22] for the pellet samples (Figure 3). No evidence of Hg was detected by XPS in any of the sorbents while monitoring the isolated but weaker Hg 4d peak, either (Figure S8 of the Supporting Information). Consequently, this study focuses on the changes in other elements important for Hg reaction chemistry after exposure to Hg sorption

Table 2. Elemental Compositions of Various Samples from Their XPS Survey Spectra

sample name	C	O	Br	Si	S(VI)[a]	S(0,SH)[a]	N	Cl	Hg	Al	Ca	Na
UTBP	87.1	10.6	0.3	0.4	0	0	0	0	0	0[b]	0[b]	1.6
UTSP	82.7	13.4	0	1.4	0.3	0.3	0	0	0	2.0	0[b]	0[b]
UTSF	89.4	4.0	0	0	0.6	6.0	0	0	0	0	0	0
TBP	48.2	36.8	0	4.1	7.1	0.2	0.8	0	0	1.1	0[b]	1.7
TSP	66.0	22.5	0	4.1	3.3	0.2	2.8	0	0	1.2	0[b]	0[b]
TSF	85.9	7.8	0	0	1.3	5.1	0	0	0	0	0	0

[a]S(VI) and S(0,SH) compositions were calculated using the ratio of each found in high-resolution scans and the total S found from the survey scan. [b]While compositions are 0.0 for survey, high-resolution scans indicate trace, non-zero values (Table S2a,b of the Supporting Information).

Table 3. Elemental Compositions of Various Samples from Their XPS Survey Spectra Normalized to 100% C

sample name	C	O	Br	Si	S(VI)[a]	S(0,SH)[a]	N	Cl	Hg	Al	Ca	Na
UTBP	100	12.2	0.3	0.5	0	0	0	0	0	0[b]	0[b]	1.8
UTSP	100	16.2	0	1.7	0.4	0.4	0	0	0	2.4	0[b]	0[b]
UTSF	100	4.5	0	0	0.7	6.7	0	0	0	0	0	0
TBP	100	76.4	0	8.5	14.8	0.3	1.7	0	0	2.3	0[b]	3.5
TSP	100	34.1	0	6.2	5.0	0.3	4.2	0	0	1.8	0[b]	0[b]
TSF	100	9.1	0	0	1.5	6.0	0	0	0	0	0	0

[a]S(VI) and S(0,SH) compositions were calculated using the ratio of each found in high-resolution scans and the total S found from the survey scan. [b]While compositions are 0.0 for survey, high-resolution scans indicate trace, non-zero values (Table S2a,b of the Supporting Information).

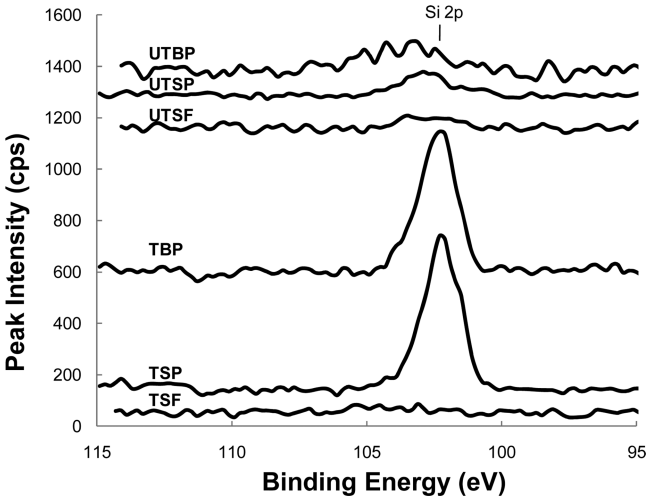

Figure 3. Compiled Si 2p/Hg 4f spectra of all untested and tested samples.

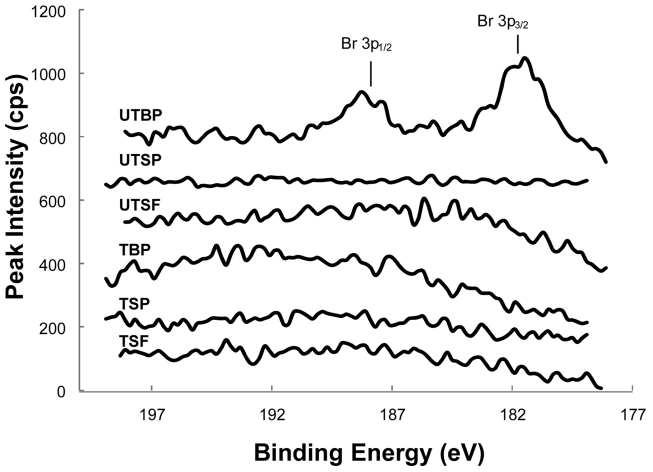

Figure 4. Compiled Br 3p spectra of all untested and tested samples.

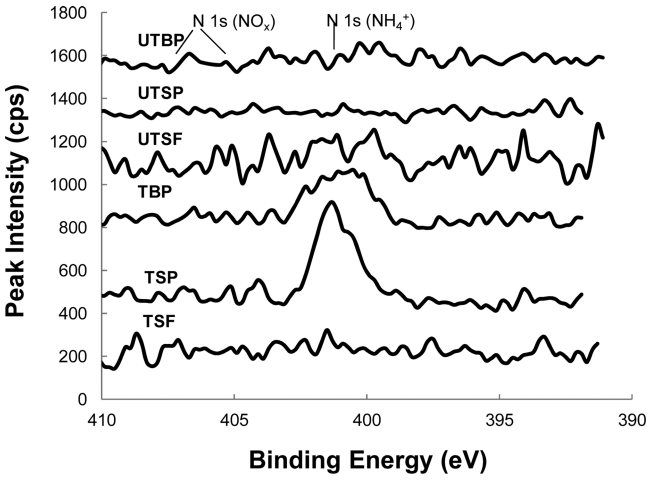

Figure 5. Compiled N 1s spectra of all untested and tested samples.

conditions; more specifically, we discuss the roles of bromine, sulfur, nitrogen, and oxygen. The XPS analysis of the untested samples will be discussed first. This will be followed by discussion on XPS analysis of tested samples. Finally, we will present insights into the Hg sorption processes on these sorbents by combining information obtained from both the XPS studies and the Hg breakthrough capacity results.

Surface Chemistry of the Untested Samples. As expected, UTBP was the only untested sample observed to contain bromine from XPS analysis. This was indicated by the presence of a Br 3p doublet at 189/182 eV (Figure 4).[23,24] The amount of bromine observed in this sample was 0.3% when normalized to carbon. No nitrogen was detected in any of the untested samples after monitoring possible N 1s lines from 398 to 407 eV (Figure 5).[25] The O 1s peak indicated the presence of 12.2, 16.2, and 4.5% normalized oxygen content for the UTBP, UTSP, and UTSF samples, respectively, with contributions possibly coming from oxidized or adventitious carbon, silica, sulfate, or metal oxide impurities (Figure S9 of the Supporting Information).

Sulfur was detected as expected on the two untested sulfur-treated samples, UTSP and UTSF, with a strong S 2p peak observed at 164 eV and a weaker one at 169 eV (Figure 6). The

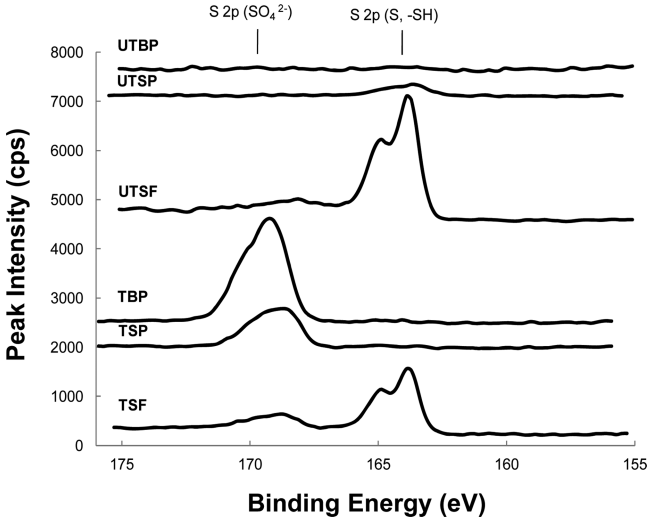

Figure 6. Compiled S 2p spectra of all untested and tested samples.

peak at 164 eV could correspond to elemental sulfur or one of the several carbon-bonded sulfur species and/or complexes such as thiophene or thiols and will be termed "reduced sulfur" hereafter, not to be confused with sulfides, which were not detected in this study.[26,27] While XPS alone cannot discern between these species,[28] elemental sulfur, thiophene, and organic thiols[29,30] have been shown to be effective for the capture of Hg from flue gases; thus, the reduced sulfur groups found on the UTSP and UTSF samples are expected to assist in the Hg capture process. More sophisticated methods of characterization would be needed to identify the chemical group with greater specificity. The peak at 169 eV is indicative of a S(VI) oxidized species such as sulfate (SO_4^{2-}),[31] which has been proposed to be a strong-binding species that is ineffective for Hg capture.[32,33] S(IV) groups such as sulfite (SO_3^{2-}) were not distinctly detected, nor were lower B.E. peaks corresponding to metal sulfides.[26]

In comparing the two sulfur-containing UTSF and UTSP samples, we observed that UTSF contained approximately 9 times more total surface sulfur (7.4% vs 0.8%) and 16 times more reduced sulfur (6.7% vs 0.4%) than UTSP when normalized to carbon. The greater fraction of reduced sulfur groups on the UTSF sample could possibly contribute to its effectiveness as a Hg capture sorbent.

Surface Chemistry of the Tested Samples. After exposure to the simulated flue gas, the surface species on each sorbent changed noticeably, leading to significant differences in the surface species among the sorbents. One important observation was that no Br was detected on the TBP sample (Figure 4). This means that the Br levels either decreased below XPS detection limits or disappeared entirely after testing. Another key change observed was the increase in the amount of sulfur present, particularly as S(VI) (Figure 6). Similar observations were also made in previous XPS studies of AC sorbents that also contained SO_2 and/or SO_3 in the flue gas.[13,14,32] The normalized amounts of S(VI) for the tested versus untested sorbents are as follows: 14.8% (TBP) vs 0.0% (UTBP), 5.0% (TSP) vs 0.4% (UTSP), and 1.5% (TSF) vs 0.7% (UTSF). Large increases in oxygen content accompanied the increase in the level of S(VI) species at a ratio of approximately 4:1, indicating that the S(VI) species formed during the capture process is SO_4^{2-}.

For the TBP sample, the only source of sulfur is SO_2 in the simulated flue gas; thus, the increase in the level of S(VI) groups and oxygen is due to the adsorption and oxidation of SO_2. The increase in the level of S(VI) in the TSP sample (5.0% vs 0.4%), which maintains a similar content of reduced sulfur groups after testing (0.3% vs 0.4%), most likely also comes from adsorbed and oxidized SO_2 from the flue gas. However, on TSF, the increase in the level of S(VI) groups (1.5% vs 0.7%) due to testing was very similar in magnitude to the decreased amount of reduced sulfur groups (6.0% vs 6.7%); one can infer that the increase in the level of S(VI) results could be from an oxidation of reduced sulfur groups rather than SO_2 adsorption and oxidation. The majority of the reduced sulfur groups on the surface of the TSF sorbent, however, remained in a reduced state even after the sorbent had been tested for 1400 h.

These results indicate a substantial difference in behavior of the TSF sample versus the TBP and TSP samples. Whereas the TBP and TSP samples clearly adsorbed large amounts of S(VI) from the SO_2 in the flue gas, XPS quantification suggests that for the TSF sample, the S(VI) produced during testing came from the oxidation of reduced sulfur originally present on the sample and not from adsorption and oxidation of SO_2 from the flue gas.

No nitrogen species were detected on the TSF sample after testing (Figure 5). However, the TBP and TSP samples exhibited nitrogen species on the surface, quantified at 1.7 and 4.2%, respectively. The nitrogen features were observed at 401 eV on the TBP and TSP and most likely arise from the NO_x in the simulated flue gas stream as no nitrogen was detected on any sample before testing. The N 1s peak location, however, does not match that for either NO (405 eV) or NO_2 (407 eV) and indicates the presence of a more reduced form of nitrogen such as ammonium,[34] as suggested by Olson.[13] The fact that the nitrogen species on the surface is in a reduced state compared to the NO_x in the flue gas suggests that the NO_x is reduced either in the flue gas or on the TBP and TSP surfaces and may participate in the Hg capture process.

Understanding the Difference in the Hg Sorption Performance between Sorbents. The Hg breakthrough data show that the tested sulfur-treated fiber sorbent, TSF, performed much better than either of the pellet samples, TSP and TBP, exhibiting more than 10 times the Hg capacity. Surface characterization of the samples by XPS before and after testing helps explain their differences in Hg capture capabilities, revealing several key differences in their surface chemistries. The presence of S(VI) groups on a surface was inversely correlated with Hg capture performance. Both the TSP and TBP sorbents, which exhibited lower rates of Hg capture, also showed a significant increase in the level of S(VI) groups on their surface after testing. XPS quantification indicates that the S(VI) likely arose from adsorption and oxidation of SO_2 from the flue gas, poisoning the surface and blocking sites for Hg adsorption.

Previously published studies discuss competition between acidic species like Hg^{2+}, SO_2, SO_3, and HCl for adsorption on basic sites of untreated AC sorbents.[13,35] This study shows evidence of similar competition, as the Br of the TBP is no longer detected and is instead replaced by large quantities of

S(VI) derived from the SO_2 in the flue gas. The other common feature of these two lower-performance sorbents is the presence of the reduced N species on the surface compared to the NO_x in the flue gas. This reduced N species could have assisted in the oxidation of SO_2 to S(VI) through chemical reactions either in the gas phase or on the sorbent surface.

The TSF had a much larger Hg capacity and saw only a small increase in the amount of S(VI) groups on the surface after testing. The proposed reason for the minimal S(VI) poisoning on the TSF was the large amount of reduced sulfur groups present on the original UTSF. The preparation of the sample introduced sulfur in amounts near saturation,[29] which likely prevented further binding of SO_2 to the surface as S(VI). Not only could the reduced sulfur groups have prevented SO_2 poisoning, but reports of strong binding of Hg by organic thiols and elemental sulfur suggest that the reduced S species could play a positive role in Hg capture. The presence of 6.0% reduced sulfur groups even after testing on the TSF is an indication of the improved Hg capacity for this sorbent. In addition, no adsorbed -NH_4^+ groups were detected on the TSF surface, consistent with the minimal adsorption and oxidation of SO_2, a potential poison. This could further explain the longevity of the TSF sorbent during breakthrough studies.

Key differences in the UTSF versus TSF sorbent chemistry compared to the UTBP versus TBP and UTSP versus TSP samples, namely a significant presence of reduced sulfur groups that may prevent poisoning of the surface by S(VI) and nitrogen-containing species, are likely responsible for the excellent Hg capture characteristics of the sulfur-treated fibers. These are important factors to consider in designing future sulfur-treated AC sorbents for Hg capture.

■ ASSOCIATED CONTENT

Supporting Information

Additional information about sorbent configuration, sample analytical methods, and data analysis; calculations explaining why Hg was not detected by XPS; and several figures depicting additional XPS spectra and pictures of reactors for pellet and fiber configurations. This material is available free of charge via the Internet at http://pubs.acs.org.

■ AUTHOR INFORMATION

Corresponding Authors

*E-mail: jaramillo@stanford.edu. Telephone: (650) 498-6879. Fax: (650) 725-7294.

*E-mail: jen.wilcox@stanford.edu. Telephone: (650) 724-9449. Fax: (650) 725-2099.

Author Contributions

A.S. and D.N.A. contributed equally to this work.

Notes

The authors declare no competing financial interest.

■ ACKNOWLEDGMENTS

We thank the Electric Power Research Institute (EPRI) for making this research possible through their generous funding. We are thankful to Dr. Massoud Rostam-Abbadi for supplying the sulfur-treated fiber samples synthesized by his group at the University of Illinois at Urbana-Champaign. We also acknowledge the contribution of Abby Kirchofer and Adam D. Jew for performing accessory experiments and for their helpful suggestions. The able guidance of Chuck Hitzman in operating the PHI VersaProbe Scanning XPS Microprobe at the Stanford Nanocharacterization Laboratory (SNL) is also much appreciated.

■ REFERENCES

(1) For additional information regarding the health effects of mercury exposure and details of the Clean Air Mercury Rule (CAMR), see http://www.epa.gov/mercury.

(2) *The Global Atmospheric Mercury Assessment: Sources, Emmision and Transport*; UNEP-Chemicals: Geneva, 2008.

(3) Kolesnikov, S. P.; Rubinskaya, T. Y.; Strel'tsova, E. D.; Leonova, M. Y.; Korshevets, I. K.; Zykov, A. M.; Anichkov, S. N. Distribution of Mercury in the Combustion Products of Coal Dust in Boilers with Liquid Slag Removal. *Solid Fuel Chem.* **2010**, *44* (1), 50−55.

(4) Granite, E. J. Overview on Mercury Control Options for Coal-Burning Power Plants. 12AIChE Annual Meeting, Pittsburgh, Nov 2, 2012.

(5) Miller, C. E.; Thomas, J.; Feeley, I.; Aljoe, W. W.; Lani, B. W.; Schroeder, K. T.; Kairies, C.; McNemar, A. T.; Jones, A. P.; Murphy, J. T. Mercury Capture and Fate Using Wet FGD at Coal-Fired Power Plants. *DOE/NETL Mercury and Wet FGD R&D* **2006**, 1−37.

(6) Olson, E. S.; Miller, S. J.; Sharma, R. K.; Dunham, G. E.; Benson, S. A. Catalytic effects of carbon sorbents for mercury capture. *J. Hazard. Mater.* **2000**, *74* (1−2), 61−79.

(7) Chang, R.; Dombrowski, K.; Senior, C. Near and Long Term Options for Controlling Mercury Emissions from Power Plants. In *7th Power Plant Air Pollutant Control Mega Symposium 2008*; Curran Associates, Inc.: Red Hook, NY, 2008.

(8) Srivastava, S. K.; Hutson, N. D.; Martin, G. B.; Princiotta, F.; Staudt, J. Control of mercury emissions from coal-fired electric utility boilers. *Environ. Sci. Technol.* **2006**, *40*, 1385.

(9) Ghorishi, S. B.; Keeney, R. M.; Serre, S. D.; Gullett, B. K.; Jozewicz, W. S. Development of a Cl-impregnated activated carbon for entrained-flow capture of elemental mercury. *Environ. Sci. Technol.* **2002**, *36*, 4454.

(10) Granite, E. J.; Pennline, H. W.; Hargis, R. A. Novel sorbents for mercury removal from flue gas. *Ind. Eng. Chem. Res.* **2000**, *39* (4), 1020.

(11) Lee, S. J.; Seo, Y.-C.; Jurng, J.; Lee, T. G. Removal of gas-phase elemental mercury by iodine- and chlorine-impregnated activated carbons. *Atmos. Environ.* **2004**, *38*, 4887.

(12) Hutson, D. N.; Attwood, B. C.; Scheckel, K. G. XAS and XPS characterization of mercury binding on brominated activated carbon. *Environ. Sci. Technol.* **2007**, *41*, 747.

(13) Olson, S. E.; Crocker, C. R.; Benson, S. E.; Pavlish, J. H.; Holmes, M. J. Surface compositions of carbon sorbents exposed to simulated low-rank coal flue gases. *J. Air Waste Manage. Assoc.* **2005**, *55*, 747.

(14) Laumb, J. D.; Benson, S. A.; Olson, E. A. X-ray photoelectron spectroscopy analysis of mercury sorbent surface chemistry. *Fuel Process. Technol.* **2004**, *90*, 1364.

(15) Miller, S. J.; Dunham, G. E.; Olson, E. S.; Brown, T. D. *Mercury sorbent development for coal-fired boilers*, Presented at Conference on Air Quality, McLean, VA, December 1−4,1998.

(16) Hsi, H.-C.; Rood, M. J.; Rostam-Abadi, M.; Chen, S.; Chang, R. Mercury Adsorption Properties of Sulfur-Impregnated Adsorbents. *J. Environ. Eng.* **2002**, *128* (11), 1080−1089.

(17) Carey, T. R.; Hargrove, O. W., Jr.; Richardson, C. F.; Chang, R.; Meserole, F. B. Factors Affecting Mercury Control in Utility Flue Gas Using Activated Carbon. *J. Air Waste Manage. Assoc.* **1998**, *48* (12), 1166−1174.

(18) Estrade-Szwarckopf, H.; Rousseau, B. Photoelectron core level spectroscopy study of Cs-graphite intercalation compounds. I. Clean surfaces study. *J. Phys. Chem. Solids* **1992**, *53*, 419.

(19) Albers, P.; Deller, K.; Despeyroux, B. M.; Prescher, G.; Schafer, A.; Seibold, K. SIMS/XPS Investigations on Activated Carbon Catalyst Supports. *J. Catal.* **1994**, *150*, 368−375.

(20) Nefedov, V. I.; Salyn, Y. V.; Solozhenkin, P. M.; Pulatov, G. Y. X-ray photoelectron study of surface compounds formed during flotation of minerals. *Surf. Interface Anal.* **1980**, *2*, 170.

(21) Humbert, P. An XPS and UPS photoemission study of HgO. *Solid State Commun.* **1986**, *60*, 21.
(22) Anwar, M.; Hogarth, C. A.; Bulpett, R. An XPS study of amorphous MoO_3/SiO films deposited by co-evaporation. *J. Mater. Sci.* **1990**, *25*, 1784.
(23) Sharma, J.; Iqbal, Z. X-ray photoelectron spectroscopy of brominated $(SN)_x$ and S_4N_4. *Chem. Phys. Lett.* **1978**, *56*, 373.
(24) Uwamino, Y.; Tsuge, A.; Ishizuka, T.; Yamatera, H. X-ray Photoelectron Spectroscopy of Rare Earth Halides. *Bull. Chem. Soc. Jpn.* **1986**, *59*, 2263.
(25) Swartz, W. E.; Alfonso, R. A. N(ls) photoelectron spectra of transition metal biguanide complexes. *J. Electron Spectrosc. Relat. Phenom.* **1974**, *4*, 351.
(26) Lindberg, B. J.; Hamrin, K.; Johansson, G.; Gelius, U.; Fahlmann, A.; Nordling, C.; Siegbahn, K. Molecular Spectroscopy by Means of ESCA II. Sulfur compounds. Correlation of electron binding energy with structure. *Phys. Scr.* **1970**, *1*, 286−298.
(27) Brion, D. Etude par spectroscopie de photoelectrons de la degradation superficielle de FeS_2, $CuFeS_2$, ZnS et PbS a l'air et dans l'eau. *Appl. Surf. Sci.* **1980**, *5*, 133.
(28) Gorbaty, M. L.; George, G. N.; Kelemen, S. R. Chemistry of organically bound sulphur forms during the mild oxidation of coal. *Fuel* **1990**, *69* (8), 1065−1067.
(29) Hsi, H.-C.; Rood, M. J.; Rostam-Abadi, M.; Chen, S.; Chang, R. Effects of Sulfur Impregnation Temperature on the Properties and Mercury Adsorption Capacities of Activated Carbon Fibers (ACFs). *Environ. Sci. Technol.* **2001**, *35* (13), 2785−2791.
(30) Liu, X.; Ruffin, M. K.; Johnson, B. Y.; Owusu, M. O. In *High Porosity In Situ Catalyzed Carbon Honeycombs for Mercury Capture in Coal Fired Power Plants*; Advances in Bioceramics and Porous Ceramics IV: Ceramic Engineering and Science Proceedings, Daytona Beach, FL, 2011; Narayan, R., Colombo, P., Eds.; Wiley: New York, 2011; pp 123−136.
(31) Christie, A. B.; Lee, J.; Sutherland, I.; Walls, J. M. An XPS study of ion-induced compositional changes with group II and group IV compounds. *Appl. Surf. Sci.* **1983**, *15* (1−4), 224−237.
(32) Presto, A. A.; Granite, E. J. Impact of Sulfur Oxides on Mercury Capture by Activated Carbon. *Environ. Sci. Technol.* **2007**, *41*, 6579−6584.
(33) Olson, E. S.; Laumb, J. D.; Benson, S. A.; Dunham, G. E.; Sharma, R. K.; Miller, S. J.; Pavlish, J. H. The Multiple Site Model for Flue Gas-Mercury Interactions on Activated Carbons: The Basic Site. *Fuel Chemistry Division Preprints* **2003**, *48* (1), 30−31.
(34) Siegbahn, K.; Nordling, C.; Fahlman, A.; Nordberg, R.; Hamrin, K.; Hedman, J.; Johansson, G.; Bergmark, T.; Karlsson, S.-E.; Lindgren, I. *ESCA: Atomic, Molecular and Solid State Structure Studied by Means of EIectron Spectroscopy*; Almqvist and Wiksells: Uppsala, Sweden, 1967.
(35) Wilcox, J.; Rupp, E.; Ying, S. C.; Lim, D.-H.; Negreira, A. S.; Kirchofer, A.; Feng, F.; Lee, K. Mercury adsorption and oxidation in coal combustion and gasification processes. *Int. J. Coal Geol.* **2012**, *90*−*91*, 4−20.